A Study of the Next WLAN Standard IEEE 802.11ac Physical Layer

NADER AL-GHAZU

KTH Electrical Engineering

Master of Science Thesis
Stockholm, Sweden 2013

XR-EE-SB 2013:001

A Study of the Next WLAN Standard IEEE 802.11ac Physical Layer

NADER AL-GHAZU

KTH Electrical Engineering

Master of Science Thesis performed at
the Signal Processing Group, KTH.
January 2013

Supervisor: Adrian Schumacher
Examiner: Joakim Jaldén

KTH School of Electrical Engineering (EE)
Signal Processing

XR-EE-SB 2013:001

Tryck: Universitetsservice AB

Abstract

This thesis studies the Physical Layer (PHY) of the new IEEE 802.11ac Wireless Local Access Network (WLAN) standard. The 11ac is built based on the 11n successful standard. The standard is expected to be completed by the end of 2013. And it promises a Very High Throughput (VHT), and robust communication. In order to achieve that, the 11ac uses more bandwidth, it employs higher numbers of Multiple-Input Multiple-Output (MIMO) spatial streams, and higher orders of modulations. The 11ac PHY frame structure is studied in details. The transmitter and receiver blocks are explained and implemented by MATLAB. Bit Error Rate (BER) and Error Vector Magnitude (EVM) simulations of the PHY were run. The effect of different Modulation and Coding Scheme (MCS), and bandwidths were studied. The performance of MIMO and Space-Time Block Coding (STBC) was investigated. The simulation results shows how the 11ac benefits from the new employed features. The created MATLAB simulation program can be used for further tests and research.

Acknowledgements

This work would not have been possible without the help, guidance, and patience of my supervisor Mr. Adrian Schumacher. I would like to thank him for giving me this opportunity to conduct my Master thesis under his supervision at Rohde & Schwarz, and for all the time he dedicated to help me.

Many thanks to my academic examiner Dr. Joakim Jaldén for his useful advice and support.

And Finally, I am very grateful to my family for their continuous love and support that they gave me.

Contents

List of Tables

List of Figures

List of Abbreviations

3GPP	3rd Generation Partnership Project
ADC	Analog to Digital Converter
ADSL	Asymmetric Digital Subscriber Line
AGC	Automatic Gain Control
AWGN	additive white Gaussian noise
BCC	Binary Convolutional Code
BER	Bit Error Rate
BPSK	Binary Phase-Shift Keying
CP	Cyclic Prefix
CRC	Cyclic Redundancy Check
CSD	Cyclic Shift Diversity
DC	Direct Current
DSP	Digital Signal Processors
DSSS	Direct-Sequence Spread Spectrum
EVM	Error Vector Magnitude
FDM	Frequency Division Multiplexing
FEC	Forward Error Correction Code
FFT	Fast Fourier Transform
FPGA	Field Programmable Gate Array
GI	Guard Interval
HDTV	High-Definition Television

HSPA+	High-Speed Packet Access plus
HT-SIG	High Throughput Signal
ICI	Inter Carrier Interference
IDFT	Inverse Discrete Fourier Transform
IEEE	Electrical and Electronics Engineers
IFFT	Inverse Fast Fourier Transform
ISI	Inter-Symbol Interference
LAN	Local Access Network
LDPC	Low-Density Parity-Check Code
L-LTF	Legacy Long Training Field
L-SIG	Legacy Signal
L-STF	Legacy Short Training Field
LTE	Long-Term Evolution
MAC	Media Access Control
MAN	Metropolitan Area Network
MCS	Modulation and Coding Scheme
MIMO	Multiple-Input Multiple-Output
ML	Maximum Likelihood
OFDM	Orthogonal Frequency-Division Multiplexing
PAPR	Peak-to-Average Power Ratio
PHY	Physical Layer
PSDU	Physical layer Service Data Unit
QAM	Quadrature Amplitude Modulation
QBPSK	Quadrature BPSK
QPSK	Quadrature Phase-Shift Keying
RMS	Root Mean Square
SIMO	Single-Input Multiple-Output

SISO	Single-Input Single-Output
SNR	Signal-to-Noise Ratios
STBC	Space-Time Block Coding
STS	Space-Time Streams
TG	Task Group
VHT	Very High Throughput
VHT-LTF	VHT Long Training Field
VHT-SIG-A	VHT Signal-A
VHT-SIG-B	VHT Signal-B
VHT-STF	VHT Short Training Field
WLAN	Wireless Local Access Network
WMAN	Wireless Metropolitan Area Networks

Chapter 1

Introduction

Wireless Local Access Networks (WLANs) had become very popular in the past decade. It replaced cable Local Access Networks (LANs) in many applications, especially for home usages. It also made it possible to provide internet services in public areas, as in airports and coffee shops. The IEEE 802.11 series of standards for WLAN have shown great success since it started in the late 1990s (also known as Wi-Fi). Nowadays, almost every laptop or smart phone has a built-in WLAN card. However, until a recent time, these WLANs have been mainly used for internet browsing, email, and other light load applications. Today, more is needed from the wireless technology; users want to be able to stream HD videos, music, or transfer large amounts of data, participate in multi-player games, or make video conferences [1]. These demands require changes to the technology. The Institute of Electrical and Electronics Engineers (IEEE) has started creating two new standards for WLAN, IEEE 802.11ac and 11ad, operating on the 5 GHz band and the 60 GHz band, respectively. The two standards are theoretically able to exceed the 1 Gbps border (Section 2.1 shows a brief introduction to the IEEE 802.11 standards). The 11ac is the new standard built on the previous successful 11n standard, it is also known as Very High Throughput (VHT). The 11ac will be able to deliver a high performance comparable to wired networks by expanding the 11n in many aspects including the following features:

- Channel bounding up to 160 MHz bandwidth
- Up to 8 spatial streams
- Higher orders of modulations up to 256-QAM

WLANs will not be limited to internet usage only; the high throughputs will expand the usage of WLANs to new fields of applications such as:

- Wireless displays (gaming, projectors)

- In home distribution of High-Definition Television (HDTV) and other contents
- Rapid upload/download of large files to/from servers
- Back-haul traffic (for 3G and 4G cellular networks)
- Campus and auditorium deployments
- Manufacturing floor automations

The 11ac standard will be able to achieve throughputs of up to 6.93 Gbps in the extreme settings case; using 160 MHz channel bandwidth, 8 spatial streams, 256-Quadrature Amplitude Modulation (QAM) and Short Guard Intervals (GIs). The 11ac will be able to coexist with the previous standards 11a and 11n which are operating on the same 5 GHz Band.

1.1 Motivation

Rohde & Schwarz® is an independent group of companies specializing in electronics. It is a leading supplier of solutions in the fields of test and measurement, broadcasting, radio monitoring and radiolocation, as well as secure communications. Established more than 75 years ago, Rohde & Schwarz has a global presence and a dedicated service network in over 70 countries. The company headquarters are in Munich, Germany.

This thesis work aims to conduct a study and analysis of the WLAN standard IEEE 802.11ac and of the current state of the standardization. A MATLAB® simulation will be developed for generating and receiving 11ac frames following the IEEE standard draft, and considering all the mandatory features and most of the optional ones. Then the simulations will run on the hardware platform in order to analyse and define requirements (e.g., spectral flatness, Error Vector Magnitude (EVM), dynamics, data rates). The simulation will be used to run performance analyses studying Bit Error Rate (BER) with the effect of different factors. Later the resources estimates and the resulting requirements for hardware and signal processing algorithms will be studied.

The simulation will be built on an existing 11n MATLAB environment. It contains the mandatory features of the 11n using a Single-Input Single-Output (SISO) system and 20 MHz channels.

1.1.1 Challenges and Hardware Requirements of 11ac

The new specification of the 11ac promises to bring higher throughput, extended ranges, and more spectrum efficiency. However these features come with a price. The 11ac introduces challenges and difficulties in designing new hardware at an affordable cost.

The 11ac specifies mandatory support for 20, 40, and 80 MHz channels, and optional contiguous 160 MHz or non-contiguous 80+80 MHz channels. This requires a new transmitter and receiver front-end for testing. The generation of an 80 MHz bandwidth signal is challenging for most signal generators and testers that are used for current WLANs due to the required high sampling rate.

The use of a high carrier frequency (in the 5 GHz band) has the advantage of being less crowded, but also brings lower propagation abilities and a shorter coverage range. And to overcome this problem, higher power is needed in the transmitter, which is limited by regulation to 10 mW/MHz in the 5 GHz band. In addition, low noise power amplifiers for the 5 GHz band have higher cost than the ones for the 2.4 GHz band.

The usage of Multiple-Input Multiple-Output (MIMO) requires multi antennas at the transmitter and receiver. The hardware should have a separate receiver connected to every antenna. In general using MIMO in a device requires more power, more complexity, and more advanced Digital Signal Processors (DSP).

The use of high modulation and coding schemes is one of the 11ac features. 256-QAM is more sensitive to noise and signal distortions, and this requires a better EVM in both the transmitter and the receiver, because the constellations points are closer to each other. The IEEE 802.11ac specifications require a -32 dB EVM for 256-QAM, in comparison to -28 dB for 64 QAM. The IQ-modulator imperfection and the power amplifier nonlinearity are sources that could affect the EVM.

1.2 Thesis Outline

The rest of the report is organized as following:

Chapter 2 contains background information about IEEE 802.11 standards, and the Wi-Fi alliance. And finally a revision of Orthogonal Frequency-Division Multiplexing (OFDM) and MIMO with a connection to the 11ac Physical Layer (PHY).

In Chapter 3, the IEEE 802.11ac PHY frame's fields are demonstrated. Followed by an explanation of the transmitter and the receiver operations in step-by-step details.

Chapter 4 demonstrates the MATLAB simulation environment, the system block structure, and the simulation considerations.

Chapter 5 presents the performance analysis results, and shows comparisons between different 11ac systems.

Conclusions and future work are stated in Chapter 6.

Chapter 2

Background

2.1 IEEE 802.11 Amended Changes

Most of the WLANs in use today are based on the IEEE 802.11 standards, which are created by the IEEE 802 LAN/MAN standards Committee. They are half-duplex systems operating on the unlicensed bands at 2.4, 3.6 and 5 GHz. They use Direct-Sequence Spread Spectrum (DSSS) and OFDM modulations techniques. Since 1999 many standard and amendments have been released, the following is a description of the popular standards.

2.1.1 802.11a

Was the first successful standard completed in 1999, it was based on an OFDM physical layer using 52 sub-carriers, it operates in the 5 GHz band and is able to reach a total throughput of 54 Mbps.

2.1.2 802.11b

Appeared on market in early 2000, it operates on the 2.4 GHz band using a DSSS system. It was able to achieve a data rate of 11 Mbps. Although the 11b has a better coverage range than 11a due to its lower carrier frequency, it suffered from interference because there are many other devices that use the same 2.4 GHz band including: microwaves ovens, baby monitors, Bluetooth and cordless phones.

2.1.3 802.11g

In mid-2003, a new standard was created, it combined the strength points of both the 11a and 11b standards. The 11g standard is based on the OFDM transmission scheme as in 11a, but operated on the 2.4 GHz band. It is fully backward compatible with the 11b and it is able to achieve a bit rate of 54 Mbps theoretically. The 11g standard was rapidly adopted by the

market, and dual band a/b/g products became the most common. Many amendments were created since then including the (802.11d, e, h, i , j), and then all merged together in 802.11ma which is also known as the base standard IEEE 802.11-2007.

2.1.4 802.11n

In 2009 a new amendment 11n was created, which employed MIMO techniques to raise the data rate significantly up to 600 Mbps. This required a multiple antenna system in both the transmitter and the receiver. It works using one to four spatial streams with 40 MHz channel bandwidth. The 11n standard operates on both the 2.4 and the 5 GHz bands, but better performance is achieved on the 5 GHz band due to the availability of non-overlapping 40 MHz channels and less radio interference. It is backwards compatible with the 11a standard when operated in the Legacy format or the Mixed Mode format (11a and 11n). But higher throughput can be achieved when operating in the Green Field format (11n only). The 11n also employed other techniques such as Space-Time Block Coding (STBC), and beam forming. The 11n products were available in the market before the completion of the standardization process.

2.1.5 802.11ac

The IEEE 802 Standards Committee created two new Task Groups (TGs) 11ac and 11ad with the goal to enhance WLANs to reach the wired networks performance. The 11ac standard operates in the 5 GHz band (does not support the 2.4 GHz Band). It should theoretically enable a data rate of at least 1 Gbps. The new specifications are built on the 11n standard, by expanding the channel bandwidth to 80 MHz and optional 160 MHz channels, in addition to using MIMO with up to 8 spatial streams, higher order of modulation scheme (256-QAM) and other optional enhanced features like beam forming. The standardization process is expected to complete by the end of 2013.

2.1.6 802.11ad

The 11ad standard operates in the unlicensed 60 GHz band. It is able to achieve a theoretical data rate of 7 Gbps, with low power consumption. This will be achieved by using wide channels of 2.16 GHz. It will support high-performance wireless implementations like HDMI and USB, extending the number of WLAN applications. The standards ia expected to reach the market by 2014.

2.2 Wi-Fi Alliance

The IEEE 802.11 standards have widespread specification and different operating modes and optional functions. This in addition to the absence of an IEEE compatibility testing facility made it difficult for manufactures to produce interoperable WLAN devices. The Wi-Fi Alliance was created to certify products that obey certain standards of interoperability. It is a trade association that was created in 1999 by a group of pioneer companies including 3Com, Cisco, Motorola and Nokia, and now it consist of more than 350 companies worldwide. They own and control the Wi-Fi CERTIFIED logo that is printed on equipment that passes their test. The main aim of the certification process to ensure interoperability, quality control, backward compatibility with previous Wi-Fi products, and innovation by introducing certifications programs for the latest technologies available in market.

2.3 OFDM

Orthogonal Frequency-Division Multiplexing is a method of digital modulation in which the available channel bandwidth is split into adjacent narrowband channels (called sub-carriers or tones), and the high-data-rate stream is split into several low-data-rate streams which are multiplexed to the subcarriers and transmitted simultaneously. The data is modulated using any form of digital data, but the most common are Binary Phase-Shift Keying (BPSK), Quadrature Phase-Shift Keying (QPSK), and QAM. The OFDM concept has been known since the late 1960s, but it was very difficult to implement OFDM transceivers with the electronics technologies that were available at that time. It only became possible to bring it to life after the industrial revolution of semiconductors and computer technologies. In, general the OFDM signal is created by assigning the digital data to sub-carriers, then using an Inverse Fast Fourier Transform (IFFT) to represent the signal in the time domain. The IFFT sorts all the signals' components into individual sine-wave elements of specific frequency and amplitude. These operations are then reversed at the receiver to retrieve the original data using a Fast Fourier Transform (FFT). The IFFT and FFT are complex mathematical operations done using DSP or Field Programmable Gate Arrays (FPGAs) in real time.

OFDM offers higher performance and benefits over the traditional single-carrier modulation techniques. The OFDM overcomes the problems associated with multipath channels; it shows high robustness to narrow-band co-channel interference, it reduces the Inter-Symbol Interference (ISI), and it can achieve spectrally efficient high data rates close to the Shannon limit.

OFDM was first used in digital radio broadcasting (Europe's DAB). It is also used in TV broadcasting (DVB-T and DVB-H), WLAN's (IEEE 802.11

a/g/n/ac standards). The Wireless Metropolitan Area Networks (WMAN) standard WiMAX, and the new 4G Long-Term Evolution (LTE) standard both use OFDM. One of the earliest successful widespread usages of a technology similar to OFDM is the Asymmetric Digital Subscriber Line (ADSL) modems. They are used for internet access using the telephone line network.

2.3.1 OFDM vs. Single-Carrier

Unlike OFDM, the single-carrier modulations transmit all the data symbols serially using one carrier frequency. These systems have several advantages over OFDM, they are less sensitive to frequency offsets and phase noise, and they avoid Peak-to-Average Power Ratio (PAPR) problems. These are the drawbacks of using OFDM, but different techniques are employed when using OFDM to overcome these problems. The single-carrier modulations main disadvantage is the multipath distortion. If a multi-path channel caused a null at the carrier frequency then the whole link will suffer causing performance degradation. A similar situation in an OFDM system would cause some sub-carriers to get distorted, not the whole link. This makes multi-carrier OFDM systems reduce the ISI and multipath distortions.

2.3.2 OFDM vs. Frequency Division Multiplexing (FDM)

In other multi-carrier (parallel data) systems such as FDM, the sub-carriers are totally separated with guard intervals to avoid Inter Carrier Interference (ICI) or cross-talk from other adjacent sub-carriers. This separation in the spectrum causes a huge waste in the frequency spectrum. An OFDM system is similar to FDM systems, except that it split the spectrum into adjacent overlapping sub-carriers, which saves a big portion of the spectrum, as shown in Figure 2.1 The reason that this became possible without causing

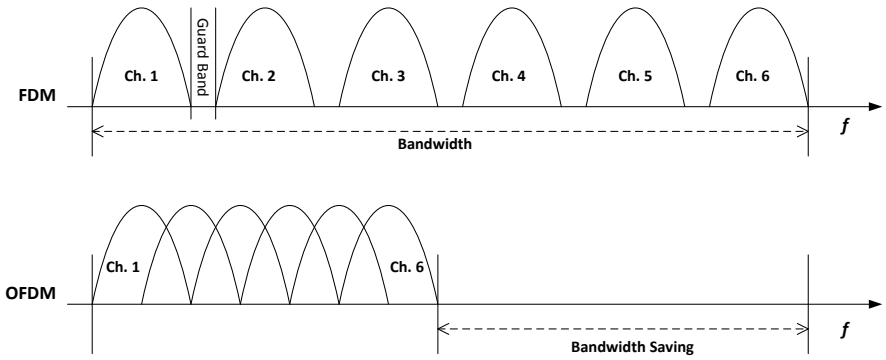

Figure 2.1: Difference between FDM and OFDM.

ICI is that the individual sub-carriers are orthogonal. This means that the signals are uncorrelated and independent over one symbol duration. In more practical terms, it means that if the sub-carriers are spaced from each other by a specific distance equal to the symbol period of the data signals, the resulting frequency response curve of the signals is such that the first nulls following the main lobe occur at the sub-carrier frequencies on the adjacent channels. Orthogonal sub-carriers all have an integer number of cycles within the symbol period, as visualised in Figure 2.2. The orthogonality prevents sub-carrier demodulators from seeing other frequencies rather than their own. This also simplifies the structure of the transmitter, unlike conventional FDM, a separate filter for each sub-channel is not required.

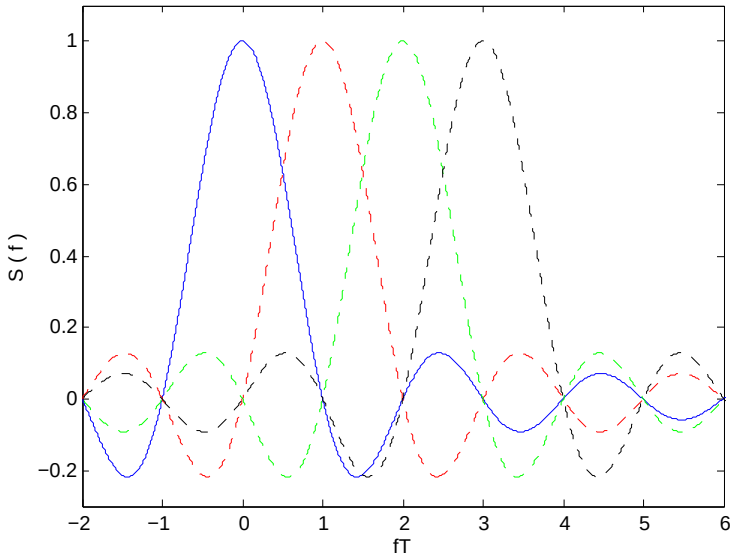

Figure 2.2: Orthogonal subcarriers in OFDM.

OFDM modulated signals are sensitive to frequency offset caused by imperfections in transceivers oscillators or Doppler shift due to movement. OFDM requires accurate frequency synchronisation between the receiver and the transmitter. A slight frequency deviation and the sub-carriers will no longer be orthogonal. This problem becomes severe with higher moving speeds, and it is difficult for the receiver to compensate for the distortion. This makes OFDM not the perfect solution for high-speed vehicle communication. Time synchronisation is enhanced by inserting a guard interval between symbols in time domain. Transmitting low-rate parallel streams made it feasible due to the relatively long duration symbols. This will reduce ISI, and eliminates the need for a pulse-shaping filter. A Cyclic Prefix (CP) is transmitted during these guard intervals; it consists of the end of the OFDM symbols copied to the guard interval. This allows the linear

convolution of the transmitted OFDM symbol with the channel to appear as circular convolution, which helps the receiver to integrate over an integer number of sinusoid cycles when it performs OFDM demodulation with the FFT.

2.3.3 OFDM in IEEE 802.11ac

The IEEE 802.11ac bandwidth is split into sub-carriers with a sub-carrier spacing of 312.4 kHz [2]. The number of sub-carriers is set to a power of two for efficient FFT operations, see Table 2.1. Most of the sub-carriers are used for carrying data samples. Few sub-carriers are assigned for pilots, which are used as a reference for phase and frequency shift corrections of symbols during transmission. These pilot sub-carriers are set apart to make a good

Table 2.1: Number of OFDM subcarriers in 11ac.

Bandwidth (MHz)	**20**	**40**	**80**	**160**
FFT Size	64	128	256	512
Number of SCs	52	108	234	468
Number of Pilot SCs	4	6	8	16
Total number of SCs	56	114	242	484
Transmission SCs	±(1–28)	±(2–58)	±(2–122)	±(6–126) ±(130–250)

estimation over the whole bandwidth. Figure 2.3 shows the pilot sub-carriers in a 20 MHz channel. The sub-carriers at the middle of the bandwidth (DC) are nulled to reduce problems in analogue baseband circuits, and the sub-carriers at the higher and lower edges of the bandwidth are nulled to avoid interference from adjacent channels.

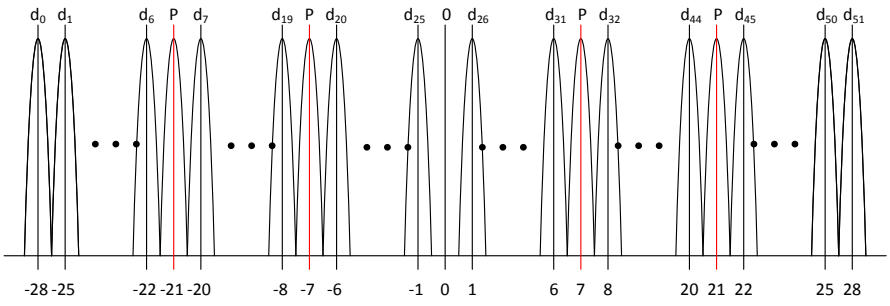

Figure 2.3: OFDM Subcarriers in 20 MHz channel in IEEE 802.11.

The OFDM symbols must be lead by a Guard Interval to provide resis-

tance to ISI, and time synchronization errors. In the IEEE 802.11 standards, the symbols duration is 4 μs , 20% of this duration (800 ns) is the GI, which carries a cyclic prefix of the signal. Considering a small symbol timing inaccuracy, this GI allows the receiver to handle a channel delay spread of 600 ns, with trade-off of symbol duration effectiveness see Figure 2.4.

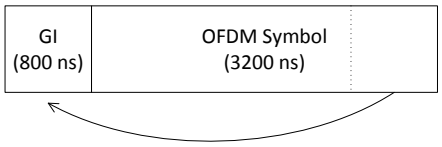

Figure 2.4: IEEE 802.11 Symbols GI.

2.4 MIMO

Multiple-Input Multiple-Output is the use of multiple antennas at both the transmitter and receiver to improve wireless communication performance. MIMO technology takes advantage of the multipath phenomenon where transmitted information bounces off walls, ceilings, and other objects, reaching the receiving antenna multiple times via different angles and at slightly different times [3]. In other words, MIMO technology takes advantage of multipath propagation to enhance the system performance Figure 2.5. It

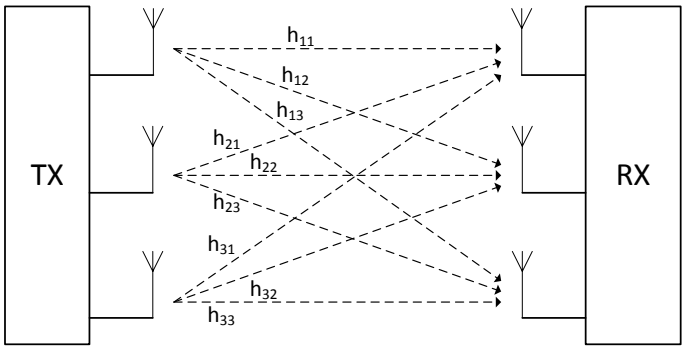

Figure 2.5: A 3x3 MIMO system.

offers significant increases in data throughput and link range without additional bandwidth or extra transmit power. MIMO is used in the WLAN 11n and 11ac standards. It is also used in other mobile radio telephone standards such as recent 3rd Generation Partnership Project (3GPP), High-Speed Packet Access plus (HSPA+) and LTE standards.

2.4.1 Spatial Multiplexing

In spatial multiplexing, high rate signals are split into multiple lower rate streams, each stream can be transmitted from a different transmit antenna using the same frequency channel. When these signals arrive at the receiver antennas with sufficiently different spatial signatures, the receiver will be able to separate these data streams into parallel channels. Spatial multiplexing is a very powerful technique for increasing channel capacity at higher Signal-to-Noise Ratios (SNR). The number of antennas in the transmitter or the receiver limits the number of possible spatial streams. The 11ac allows up to 8 spatial streams. Independent data streams can be multiplexed to these spatial streams. And the antennas have to be spaced in distances in the order of the wavelength, usually half a wavelength (2.7 cm in the 5 GHz band). The usage of spatial streams is dependent on the MIMO channel, which can be modelled as a matrix for each sub-carrier as in (2.2).

$$R(k) = H(k)S(k) + N(k) \tag{2.1}$$

$$H(k) = \begin{bmatrix} h_{1\,1}(k) & \dots & h_{1\,M}(k) \\ \vdots & \ddots & \vdots \\ h_{N\,1}(k) & \dots & h_{N\,M}(k) \end{bmatrix} \tag{2.2}$$

where each element $h_{i,j}$ of $H(k)$ is a complex number representing the channel gain and phase of sub-carrier k, $R(k)$ is the received signal, $S(k)$ is the transmitted signal, and $N(k)$ is the additive white Gaussian noise (AWGN). These channel elements can be estimated at the receiver using the preambles described later, then used to equalise the rest of the received symbols. Finding a solution to the channel matrix requires a minimum rank of M, which means that the matrix $H(k)$ should consist of at least M linearly independent unique rows [4]. This requires the MIMO channels between the transmitter and receiver to have a dense multipath reflections or scattering. This is usually the case in indoor systems, and also enhanced by appropriate spacing of antennas. This is usually considered as sources of distortion in other communication systems, where in MIMO, it is the key of making everything work.

2.4.2 STBC

Space-Time Block Coding is a technique used in wireless communications to transmit multiple copies of a data stream across a number of antennas and to use the various received versions of the data to improve the reliability of data transfer. The transmitted signal usually travels through a difficult environment with scattering, reflection, refraction and other types of distortion, and then it may also be further corrupted by interferences or thermal noise in the receiver. This means that some of the received copies of the

data will be less distorted than others. This redundancy results in a higher chance of being able to use one or more of the received copies to correctly decode the received signal. In fact, STBC combines all the copies of the received signal in an optimal way to extract as much information from each of them as possible.

In 11ac STBC can be used to expand the spatial streams to double their number of space-time streams. So it can only be used to expand 1, 2, 3 and 4 spatial streams into 2, 4, 6, and 8 space-time streams, respectively, unlike 11n where all combinations of STBC expansions are possible [5]. Alamouti's scheme is used because it is the only scheme that provides full transmit diversity gain with low complexity for a system with two antennas. When applied to a system with 1 to 4 spatial streams, each spatial stream is expanded separately using Alamouti's code as follows, for two inputs x_1 and x_2 (in time domain), the first spatial stream transmits the symbols x_1 and x_2 in their original order, the second spatial stream transmits $-x_2^*$ and x_1^* which are the space-time coding [6] (where $*$ stands for the conjugate). The transmitter outputs are as in (2.3).

$$y_1 = \begin{bmatrix} x_1 \\ -x_2^* \end{bmatrix}, \quad y_2 = \begin{bmatrix} x_2 \\ x_1^* \end{bmatrix} \tag{2.3}$$

The received symbols will be as in (2.4)

$$\begin{aligned} r_1 &= \begin{bmatrix} h_{11} & h_{12} \end{bmatrix} \cdot \begin{bmatrix} x_1 \\ -x_2^* \end{bmatrix} + n_1 \\ r_2 &= \begin{bmatrix} h_{21} & h_{22} \end{bmatrix} \cdot \begin{bmatrix} x_2 \\ x_1^* \end{bmatrix} + n_2 \end{aligned} \tag{2.4}$$

The receiver can recover the transmitted data with linear processing. The low complexity along with the full diversity gave Alamouti's code great advantages over other high order STBC codes even though they could achieve better BER rates.

Chapter 3

IEEE 802.11ac

The 11ac standard reuses much of the previous legacy 11n and 11a standards. It uses the same sub-carriers structure in the 20 and 40 MHz bandwidth, and an extension of these is used for the higher channel bandwidths (see Table 2.1). A legacy preamble is transmitted on every 20 MHz of the bandwidth so that all 802.11 devices can synchronise to the packets. The effect of the PAPR problem is reduced by the phase rotation method [7]; The constellations in the upper 20 MHz sub bands are rotated relative to the constellations in the lower sub bands, as shown in Table 3.1.

Table 3.1: Bandwidth rotation parameters.

Bandwidth (MHz)	**Rotated Sub Band**	**Rotation Value**
20	—	—
40	$k \geq 0$	90°
80	$k \geq -64$	180°
160	$-190 \geq k \geq -1$ and $k \geq 64$	180°

The PHY of the 802.11 interfaces to the Media Access Control (MAC) through an extension of the PHY generic interface. The interface includes TXVECTOR and the RXVECTOR. These includes all the necessary parameters for the PHY to generate, transmit or receive a data frame, some of them are transmitted in a compact form to the receiver in the preambles. The TXVECTOR supplies the PHY with the transmission parameters, and the RXVECTOR allows the PHY to inform the MAC of the received parameters.

3.1 PHY Frame Structure

The VHT PHY frame consists of a legacy preamble, a VHT preamble and the data payload. The symbol blocks are shown in Figure 3.1. The legacy

preamble consists of a Legacy Short Training Field (L-STF), a Legacy Long Training Field (L-LTF), and a Legacy Signal (L-SIG) field. These fields are the same as the ones in 11a and 11n (legacy and mixed formats) preambles. They allow all 802.11 devices to synchronize to the data frame, and avoid interference of other stations. Then follows the VHT preambles, VHT Signal-A (VHT-SIG-A) field, VHT Short Training Field (VHT-STF), VHT Long Training Field (VHT-LTF), VHT Signal-B (VHT-SIG-B) field and finally the DATA symbols. The following sections give a brief explanation of the preamble fields.

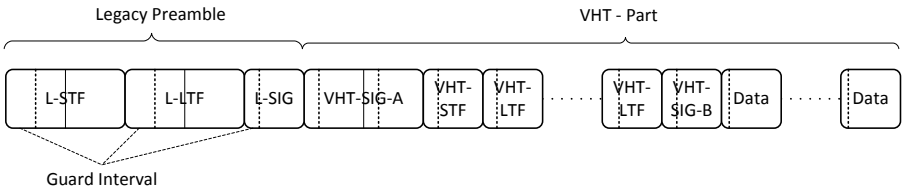

Figure 3.1: VHT PHY frame fields.

3.1.1 L-STF

The L-STF is used for Automatic Gain Control (AGC), time synchronization and frequency offset correction. This field consist of 12 sub-carriers for the 20 MHz bandwidth, which carry the values of $1 + j$ and $-1 - j$. In time domain the signal appears as a 10 times repeated signal. For larger bandwidths, the L-STF is just repeated on every bandwidth with the proper rotation as in Table 3.1.

3.1.2 L-LTF

The L-LTF is the used for the main channel estimation in the 11a, while in the 11ac it is only used to for channel estimation in order to decode the L-SIG and the following field of VHT-SIG-A. This field consist of 52 sub-carriers for the 20 MHz channel as in (3.1).

$$\begin{aligned} L_{-26,26} = \{&1, 1, -1, -1, 1, 1, -1, 1, -1, 1, 1, 1, 1, 1, 1, -1, -1, 1, \\ &1, -1, 1, -1, 1, 1, 1, 1, 0, 1, -1, -1, 1, 1, -1, 1, -1, 1, \\ &-1, -1, -1, -1, -1, 1, 1, -1, -1, 1, -1, 1, -1, 1, 1, 1, \} \end{aligned} \tag{3.1}$$

For larger bandwidths, the L-LTF is constructed of repeated copies of the one shown in (3.1). Two OFDM symbols of L-LTF are used with a double GI placed in the first symbol.

3.1.3 L-SIG

The L-SIG is the last symbol of the legacy preamble, it originally carries the data rate and length of the rest of the packet in octets (8-bits) in 11a frames as shown in Figure 3.2, the 11a devices can calculate the time required for a packet to be transmitted before they try to use the channel. In 11ac

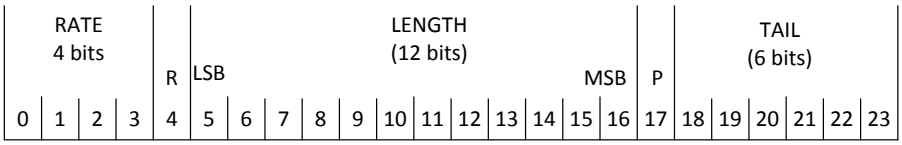

Figure 3.2: L-SIG field bit assignment.

the packet length is limited to 5.484 ms regardless of the Modulation and Coding Scheme (MCS) used. The L-SIG data rate field is always set to 6 Mbps, and the length field is set to a value calculated from the number of symbols as in (3.2). This length value forces legacy devices to wait until the transmission of the packet is over. The length field can hold a maximum value of 4095. This value translates in 11a devices into a total time frame equal to 5.464 ms, which is slightly less than the maximum DATA field length defined in 11ac. In practice most transmitted frames in all 802.11 devices do not exceed 3 ms. The actual length of the DATA is defined in an other VHT field.

$$\text{Length} = (N_{Symbols} - 6) \times 3 \tag{3.2}$$

where $N_{Symbols}$ is the number of OFDM DATA field symbols.

3.1.4 VHT-SIG-A

The VHT-SIG-A is the first VHT field, it consist of two symbols that carries the required parameters for an 11ac station to decode the rest of the burst[1]. The VHT-SIG-A consist of two symbols each containing 24 bits. The first symbol is BPSK modulated and encoded using a Binary Convolutional Code (BCC) with a coding rate of $\frac{1}{2}$, this causes 11n stations to treat the burst as a legacy 11a burst. The second symbol is rotated by 90°(Quadrature BPSK (QBPSK) modulated) to enable 11ac stations to auto detect the burst at the receiver, see Figure 3.3 The first symbol VHT-SIG-A1 contains bits to specify the channel bandwidth, the group ID, the number of space-time streams used, and another field for multi-user burst support.

The VHT-SIG-A2 contains a field for indicating whether a short GI is used or not, a field for the type of encoding used; either a BCC or a Low-Density Parity-Check Code (LDPC). Then a field of 4 bits is used for the

[1]A similar field exists in the 11n case, namely the High Throughput Signal (HT-SIG)

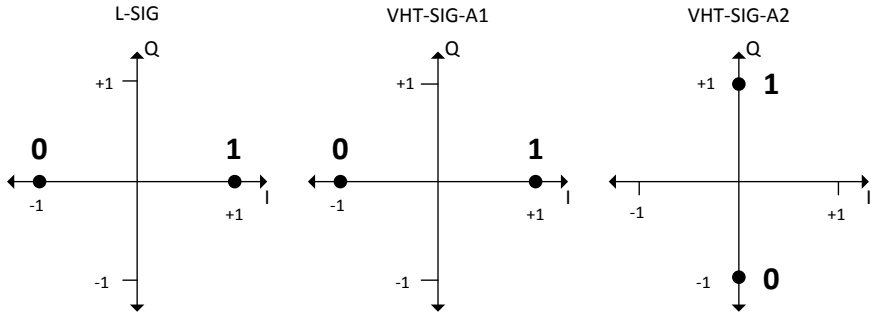

Figure 3.3: Constellations of L-SIG and VHT-SIG-A symbols.

MCS in the single-user case and for indicating the type of encoder per user in a multi-user case. This is followed by a bit for beam forming, 8 bits for Cyclic Redundancy Check (CRC), and finally 6 tail bits. All the SIG symbols contain reserved bits that are set to a fixed value. Figure 3.4 shows a diagram of the VHT-SIG-A symbols structure. The VHT-SIG-A is repeated

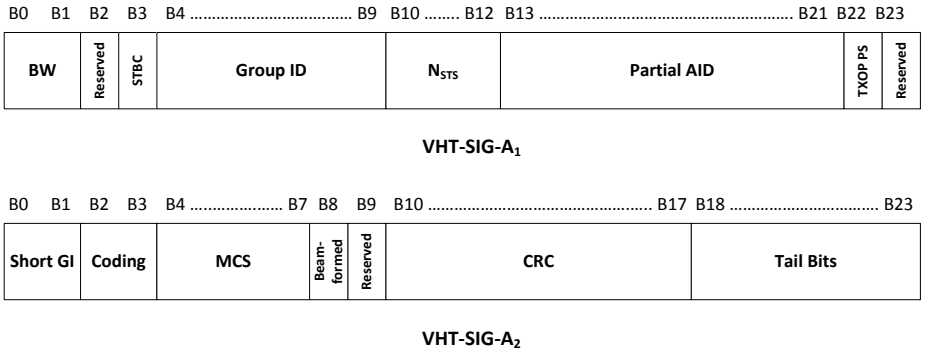

Figure 3.4: VHT-SIG-A frame structure for Single-User.

for every 20 MHz of bandwidth (with proper tone rotation) and for every transmitted chain. It has a long GI inserted before each symbol and follows the transmitting procedure of DATA symbols except for scrambling. The receiver uses channel estimation from the L-LTF to decode the VHT-SIG-A and read its values, before it goes through the receiving process of the DATA symbols.

3.1.5 VHT-STF

The VHT-STF is used for automatic gain control in the MIMO transmission and for fine tuning of the time synchronisation. It is similar to the L-STF and consists of a sequence of tones that are set to values of $+1+j$ and $-1-j$. These tones are carried on a small portion of the sub-carriers, while the other sub-carriers are all set to zero. The sequences for the 20 MHz and the 40 MHz bandwidths are identical to the ones in the 11n as shown in (3.3) and (3.4).

$$\begin{aligned} S_{-26,26} = \sqrt{\frac{1}{2}}\{&0,0,1+j,0,0,0,1+j,0,0,0,-1-j,0,0,0,-1-j,\\ &0,0,0,1+j,0,0,0,0,0,0,0,-1-j,0,0,0,-1-j,0,\\ &0,0,1+j,0,0,0,1+j,0,0,0,1+j,0,0,0,1+j,0,0\} \end{aligned} \tag{3.3}$$

$$S_{-58,58} = \{S_{-26,26},0,0,0,0,0,0,0,0,0,0,0,0,S_{-26,26}\} \tag{3.4}$$

The VHT-STF frequency sequence for the 80 MHz bandwidth is using the $S_{-58,58}$ as shown in (3.5).

$$VHTS_{-122,122} = \{S_{-58,58},0,0,0,0,0,0,0,0,0,0,0,0,S_{-58,58}\} \tag{3.5}$$

And for the 160 MHz bandwidth it uses the $VHTS{-}122,122$ as shown in (3.6)

$$\begin{aligned} VHTS_{-250,150} = \{&VHTS_{-122,122},0,0,0,0,0,0,\\ &0,0,0,0,0,VHTS_{-122,122}\} \end{aligned} \tag{3.6}$$

The VHT-STF uses long GI and is repeated on all every space-time stream.

3.1.6 VHT-LTF

The VHT-LTF is used by the receiver for MIMO channel estimation, and equalizing the DATA fields. The VHT-LTF consists of a sequence of 1s and -1s similar to the ones used in the L-LTF, except that there are less zero sub-carriers. The transmitter inserts VHT-LTFs prior to the DATA fields in every space-time stream. The number of space VHT-LTFs depends on the number of space-time streams as shown in Table 3.2. These fields are

Table 3.2: Number of VHT-LTF fields.

Number of STS	1	2	3	4	5	6	7	8
Number of VHT-LTFs	1	2	4	4	6	6	8	8

encoded over space and time using the orthogonal matrix in (3.7). This

matrix is used for 1 to 4 streams, and other extended matrices are used for higher number of streams.

$$P_{VHTLTF} = \begin{bmatrix} 1 & -1 & 1 & 1 \\ 1 & 1 & -1 & 1 \\ 1 & 1 & 1 & -1 \\ -1 & 1 & 1 & 1 \end{bmatrix} \tag{3.7}$$

Every row represents a space-time stream, and the VHT-LTFs are multiplied by the matrix elements as shown in Figure 3.5. Unlike 11n, the pilots' sub-carriers are multiplied by the first row of the P_{VHTLTF} matrix and are identical on all streams. This allows for correcting phase offsets in the DATA field symbols before doing channel estimation. The VHT-LTF fields use the long GI.

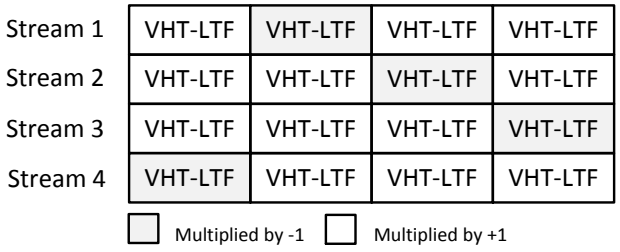

Figure 3.5: VHT-LTF multiplication with P_{VHTLTF} matrix.

3.1.7 VHT-SIG-B

VHT-SIG-B is the third signal field that contain information about the burst; it is one symbol with BPSK modulation. The VHT-SIG-B carries information about the length of the transmitted DATA and the MCS per user for the multi-user case. For the single-user case it only informs the receiver of the length of the transmitted DATA (see Figure 3.6). The number of bits in the length field varies by bandwidth as shown in Figure 3.7. This allows the length field to hold the maximum value that can maintain the 5.464 ms DATA field. The VHT-SIG-B is repeated on all space-time streams and multiplied by the first column of the P_{VHTLTF} matrix in (3.7), hence it can be equalized by using the channel estimation calculated form the first symbol of the VHT-LTF, and does not require MIMO channel estimation.

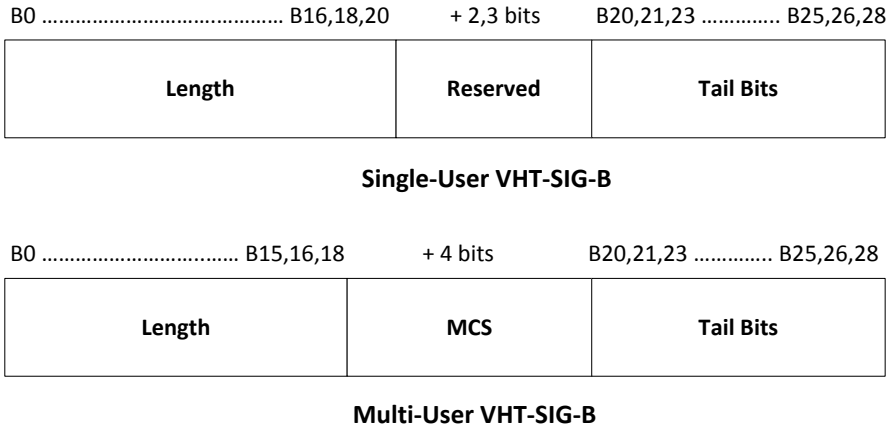

Figure 3.6: VHT-SIG-B for Sing-User and Multi-User.

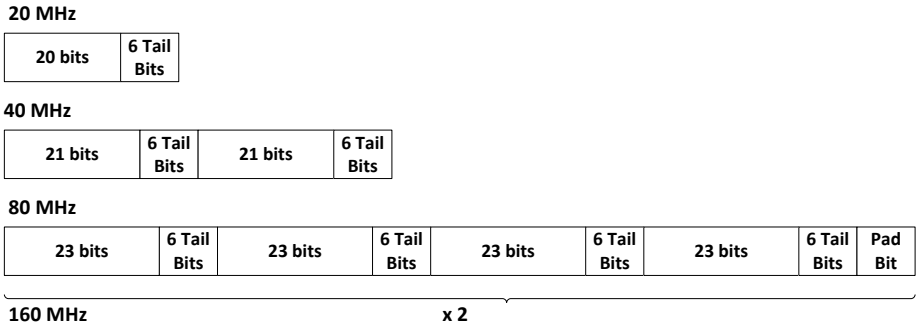

Figure 3.7: VHT-SIG-B for different bandwidths.

3.1.8 DATA field

The DATA field consist of a variable number of OFDM symbols that carry the Physical layer Service Data Unit (PSDU) which is basically the PHY payload to be transmitted. The number of transmitted symbols in the DATA field is determined by the L-SIG field. The first DATA field symbol contains the SERVICE field, the SERVICE field carries the scrambler initialisation code, and a CRC calculated from the VHT-SIG-B excluding the tail bits as shown in Figure 3.8. All the fields go through different numbers of processes explained in the next section.

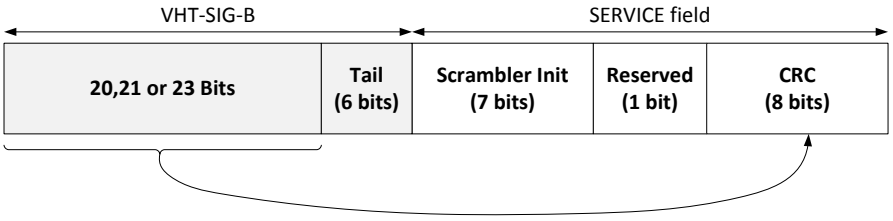

Figure 3.8: The SERVICE field and its relation with VHT-SIG-B.

3.2 Transmitter Structure

The transmitter consists of different blocks of operations. The DATA field is generated by passing the PSDU through all the blocks of the transmitter. A block diagram of the transmitter structure is shown in Figure 3.9. The preamble fields of the VHT frame uses subsets of the transmitter blocks. Each block function will be explained in the following.

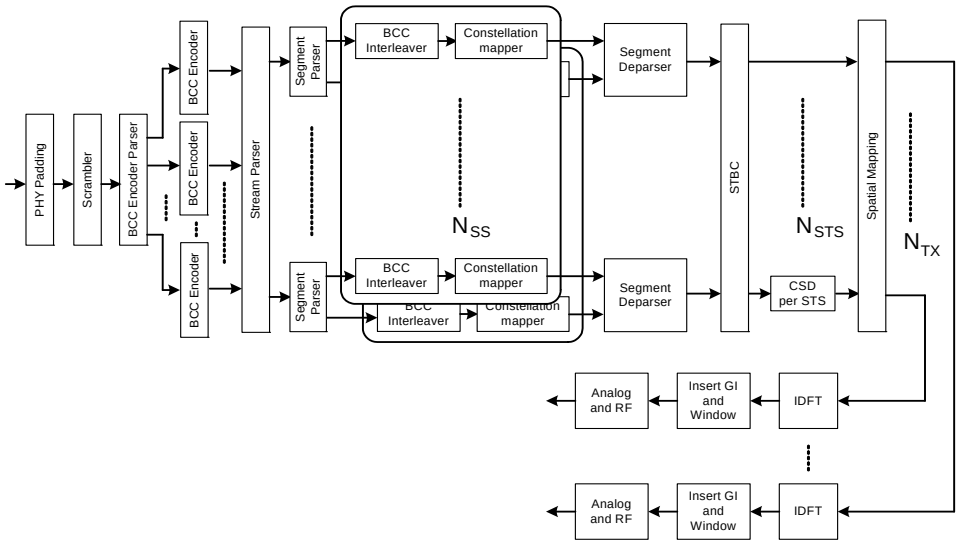

Figure 3.9: Transmitter block diagram of the DATA field with BCC encoders [2].

3.2.1 PHY Padding

The first block of the transmitter is the PHY padding, it adds a number of zero bits to the end of the frame to ensure an integer number of OFDM symbols. The MAC creates the initial padding, and the PHY adds 0–7

bits per user. The number of bits for a single user using BCC encoders is calculated according to the equation (3.8).

$$N_{PAD} = N_{SYM}N_{DBPS} - 8 \cdot \text{PSDU}_{Length} - N_{Service} - N_{Tail}N_{ES} \quad (3.8)$$

where N_{PAD} is the number of padding bits, N_{DBPS} is the number of data bits per OFDM symbol, $N_{service}$ is the number of bits in the SERVICE field, N_{tail} is the number of tail bits (6 bits), and N_{ES} is the number of encoders in the transmitter.

3.2.2 Scrambler

The scrambler manipulates the data stream to a seemingly random output stream; this avoids long sequences of bits with the same value, and adds desired properties to the transmitted data stream. The DATA field, composed of SERVICE, PSDU, tail and pad parts, shall be scrambled with a length-127 frame-synchronous scrambler. The main feature of the frame-synchronous scrambler is that a single transmission error will only produce a single error after the receiver descrambler [8]. The octets of the PSDU are scrambled using the generator polynomial shown in (3.9) and illustrated in Figure 3.10 where the leftmost bit is used first [5].

$$S(x) = x^7 + x^4 + 1 \quad (3.9)$$

The same scrambler is used in the transmitter and the receiver and it should always be initialised with a non-zero state.

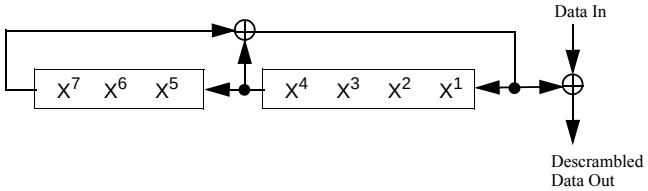

Figure 3.10: Data scrambler [5].

3.2.3 Forward Error Correction Code (FEC) encoders

The DATA field in the 11ac should be encoded using one of two types of FEC encoders; the BCC and the LDPC, but only the BCC encoder was supported in the simulations of this thesis, because the LDPC has not got much traction yet for WLAN. The employed BCC encoder has a constrain length $K = 7$ and it uses the industry-standard generator polynomials described with $g_0 = 133$ and $g_1 = 171$, of a coding rate R = $\frac{1}{2}$ as shown in Figure 3.11. Different MCSs require higher coding rates of R = $\frac{2}{3}, \frac{3}{4}$ and $\frac{5}{6}$, these rates

are achieved using puncturing. Puncturing is a process where some of the redundant encoded bits are removed in the transmitter in a specified pattern (reducing the number of transmitted bits and increasing the coding rate). At the receiver side, dummy zero bits are inserted in the decoder to replace the removed bits. The tail bits appended to every encoder input are not encoded.

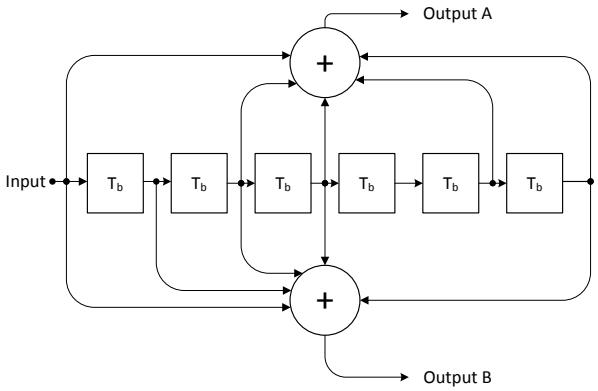

Figure 3.11: BCC encoder block diagram.

3.2.4 BCC encoder parser

In the 11ac, up to six BCC encoders have to be used to handle the encoding process at high data rates. The number of BCC encoders used is determined by the data rate which is dependant on the MCS, bandwidth and the MIMO order. When multiple BCC encoder are used, an encoder parser is needed; It divides the scrambled bits of the DATA field among the different BCC encoders in a round-robin scheduling fashion.

3.2.5 Stream parser

The bit streams at the output of the FEC encoders go through another process known as stream parsing. First they are divided into small blocks of bits, and then re-arranged into spatial streams, which is the first representation of the the MIMO streams. The number of spatial streams N_{SS} ranges from one up to eight, but in order to limit the complexity only one up to four were supported in this simulation. More details about the stream parser and the related calculations are found in [2].

3.2.6 Segment parser and segment deparser

The segment parser is only used in the case of contiguous 160 MHz or non-contiguous 80+80 MHz bandwidths. Where every spatial stream is split into two frequency segments, and every segment carries the processes of BCC Interleaving, Constellation mapper and Pilot insertion as a separate 80 MHz system. The segment deparser recombines the two frequency segments back into one frequency segment (see Figure 3.9). This only applies for 160 MHz bandwidth case, and not the 80+80 MHz case.

3.2.7 BCC Interleaver

In order to improve the performance of the system, the BCC encoded data bits are interleaved. In most communication channels errors occur in bursts rather than in independent bits. If the number of errors in a code word is greater than the BCC's error correcting capability, the receiver will not be able to recover the original transmitted data. Interleaving helps overcoming this problem by shuffling the data bits in different code words creating a better uniform distribution of the errors.

In 11ac, the interleaving is done separately for every OFDM symbols. It is done in three steps of permutations. The first ensures that adjacent codded bits are mapped into non-adjacent sub-carriers. The second permutation ensures that adjacent bits are distributed into less and more significant bits of the constellation. Finally the third permutation is called frequency rotation, it is only applied when more than one spatial stream exists. The equations for permutation are described in [2, 5].

3.2.8 Constellation mapper

The modulations process is done separately for every spatial stream. The interleaved serial data bits are arranged in groups of 1, 2, 4, 6, or 8 bits and converted into complex numbers representing a BPSK, QPSK, 16-QAM, 64-QAM, or 256-QAM constellation points respectively. The constellations are Grey-coded and normalized by the factor K_{MOD} shown in Table 3.3. Every

Table 3.3: Modulation schemes normalizing factor.

Modulation	$\mathbf{K_{MOD}}$
BPSK	1
QPSK	$1/\sqrt{2}$
16-QAM	$1/\sqrt{10}$
64-QAM	$1/\sqrt{42}$
256-QAM	$1/\sqrt{170}$

constellation point is mapped into a data sub-carrier, different bandwidths

have different numbers and order of data sub-carriers (see Table 2.1). The modulated symbols should be scaled by a factor $\sqrt{N_{Field}^{Tone}}$ dependant on the bandwidth and the PHY field being processed.

3.2.9 Pilot insertion

Pilots are BPSK modulated sequences, carried by OFDM symbol, in specific sub-carriers that are dedicated for pilots (see Table 2.1). Pilots are used for adding robustness against frequency offset and phase noise. This is done by a secondary channel estimation and correction in the receiver for every OFDM symbol. To prevent generating spectral lines, the pilots are generated as a pseudo-binary sequence that is known for the receiver.

For example, in the 20 MHz case, the bandwidth is divided into 64 sub-carriers, 4 of them are assigned for pilots (namely -21, -7, 7, 21). The sequence {1,1,1,-1} is inserted into these sub-carriers for the first OFDM symbol, then for the following symbol, the same sequence is used but after a cyclic rotation and a multiplications with the polarity controlling sequence $p_n = 1, 1, 1, 1, -1, -1, -1, 1, \ldots$ which consists of 127 elements repeated to extend to the total number of symbols. Pilots are inserted in the DATA field symbols in addition to all the SIG fields. Unlike 11n, the pilots in all the streams of a MIMO signal are identical.

3.2.10 Tone rotation

When using bandwidths higher than 20 MHz, the preamble fields are replicated over multiple 20 MHz segments of the bandwidth with proper tone rotations as shown in Figure 3.12, the parameters for rotation were shown in Table 3.1.

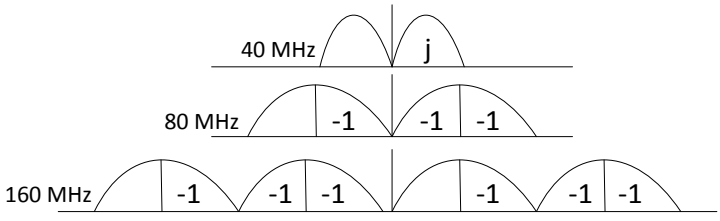

Figure 3.12: Tone rotation for different bandwidths.

3.2.11 STBC encoder

The STBC encoder improves the reliability of the the data transfer and enhance error robustness. It employs optional transmission techniques to expand the spatial streams doubling them into a number of Space-Time

Streams N_{STS}. More details are given in subsection 2.4.2. If the STBC encoder is bypassed, then direct mapping will be used, and N_{STS} will be equal to N_{SS}.

3.2.12 Cyclic Shift Diversity (CSD)

Cyclic shifts are applied to prevent unintended beam forming when correlated signals are transmitted in multiple space-time streams. Different shift values are applied to the preamble fields (pre-VHT) and the DATA field (VHT), Table 3.4 shows the values for up to four space-time streams.

Table 3.4: CSD values for pre-VHT and VHT fields.

$\mathbf{N_{STS}}$	Shift values for STS n (ns)							
	pre-VHT				**VHT**			
	1	2	3	4	1	2	3	4
1	0	-	-	-	0	-	-	-
2	0	-200	-	-	0	-400	-	-
3	0	-200	-100	-	0	-400	-200	-
4	0	-50	-100	-150	0	-400	-200	-600

3.2.13 Spatial mapper

The spatial mapper expands the space-time streams into a number of transmit chains N_{TX}, if not used then N_{TX} will be equal to N_{STS} and every space-time stream is transmitted through a separate antenna. It could also be used to simply duplicate the space-time streams to utilise more antennas, expanding the N_{STS} into a larger N_{TX} as done in this simulation. The spatial mapper can be represented by the steering matrix Q_k with N_{TX} rows and N_{STS} columns for sub-carrier k, the Q_k matrix is not limited in the 11ac standard and it can be set to any matrix, for example:

- A direct mapping identity matrix.
- A CSD matrix representing cyclic shifts in time domain.
- Hadamard matrix or the Fourier matrix used for indirect mapping.
- Different spatial expansion over sub-carriers used for smoothing.
- A beam forming matrix, where Q_k is any matrix that improves the reception in the receiver based on knowledge of the channel [5].

Whenever a spatial mapper is used to expand the space-time streams, each stream is scaled with the normalization factor $\sqrt{N_{STS}/N_{TX}}$.

3.2.14 IDFT, GI insertion and Windowing

The Inverse Discrete Fourier Transform (IDFT) converts a block of constellation points to a time domain block using IFFT as explained in section 2.3. The GI insertion prepends to the symbol a circular extension of itself, more details are shown at the end of subsection 2.3.3. Windowing is used to optionally smooth the edges of each symbol to increase spectral decay.

3.3 Receiver Structure

The receiver is designed to retrieve the transmitted PSDU from the received air signal. It consists of several connected blocks, the first parts of the receiver are mainly to detect the burst, synchronise, estimate the channel, and equalize the symbols, while the remaining of the receiver reverse the processes of the transmitter. A block diagram of the implemented receiver is shown in Figure 3.13. The following subsections explain the main receiver blocks in more details.

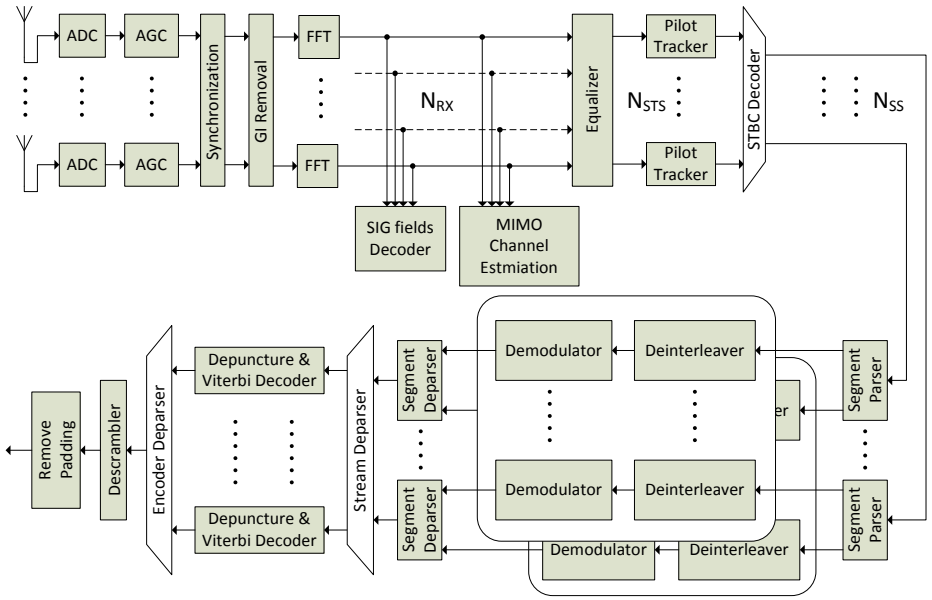

Figure 3.13: Receiver block diagram.

3.3.1 Detection and Synchronisation

The received analog signal is first sampled, converted to a digital signal by an Analog to Digital Converter (ADC), then the gain is adjusted for an appropriate input signal level using an AGC. At this level the data streams

are the inputs of every antenna and they are processed separately. A sum of signal streams can be used for the synchronization.

A burst detector benefits from the VHT-STF field. It is able to recognize a WLAN burst using normalized delay correlation [9]; that is done by running a continuous convolution for part of the received signal with a delayed version of it. When the correlation value exceeds a certain threshold, a set of other tests follows, checking some characteristics in the received signal and its power profile, if all passed then a WLAN burst is detected, a block diagram of the signal detection algorithm is shown in Figure 3.14.

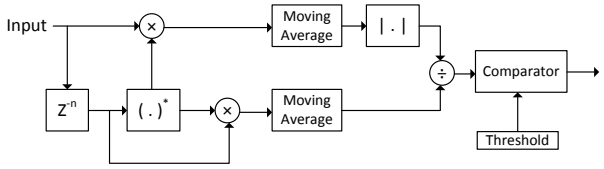

Figure 3.14: A block diagram of the signal detection algorithm.

If a WLAN burst is detected, then the falling edge of the moving average of the normalized delay correlation is used to set a pointer to the first OFDM symbol boundary (Time-Synchronisation) [10, 11]. Further fine Time-Synchronisation could be done using the VHT-STF field.

The frequency offset is also estimated from the VHT-STF and corrected for the whole data stream (Frequency-Synchronisation). The stream is then divided into symbols, the GI is removed, and then brought to the frequency domain by passing an FFT operation.

3.3.2 Channel estimation

A SIGNAL field decoder uses the L-LTF to pre-estimate the channel and decode the L-SIG and VHT-SIG-A fields (in the 11ac case), from which it extracts the RXVECTOR. The RXVECTOR contains information about the received burst, it is used to calculate all the required parameters for the remaining processes of the receiver. These fields were modulated and transmitted as legacy fields (compatible with 11a) and therefore no MIMO channel estimation is required until this point.

The MIMO channel estimation is done using the VHT-LTF fields. As explained in subsection 3.1.6, these training symbols are transmitted on every stream with different polarities making them orthogonal to each other. The receiver is able to evaluate the channel estimation for every sub-carrier separately. Let $\hat{h}_{ij}(k)$ be the channel estimation for the path between antenna i and the transmitted space-time streams j for sub-carrier k. Then

the channel estimation is represented by the $N_{RX} \times N_{STS}$ matrices series,

$$\hat{H} = [\ \hat{H}(1), \ldots, \hat{H}(k), \ldots, \hat{H}(N_{SC})] \tag{3.10}$$

where $\hat{H}(k)$ is the estimated channel matrix for sub-carrier k shown in (3.11) and N_{SC} is the total number of data sub-carriers in an OFDM symbol.

$$\hat{H}(k) = \begin{bmatrix} \hat{h}_{1\,1}(k) & \ldots & \hat{h}_{1\,N_{STS}}(k) \\ \vdots & \ddots & \vdots \\ \hat{h}_{i\,1}(k) & \ldots & \hat{h}_{i\,N_{STS}}(k) \\ \vdots & \ddots & \ldots \\ \hat{h}_{N_{RX}\,1}(k) & \ldots & \hat{h}_{N_{RX}\,N_{STS}}(k) \end{bmatrix} \tag{3.11}$$

$\hat{h}_{i\,j}(k)$ is evaluated using a Maximum Likelihood (ML) estimation algorithm [12]. Let $L_{n\,i}(k)$ be the n^{th} received VHT-LTF symbol by the receiver antenna i, then for a single space-time stream (e.g., SISO or SIMO system),

$$\hat{h}_{i\,1}(k) = \frac{L_{1,i}(k)}{VHTLTF(k)} \tag{3.12}$$

and for a system where $N_{STS} = 2$ (e.g., 2×2 MIMO system),

$$\begin{aligned} \hat{h}_{i\,1}(k) &= \frac{L_{1,i}(k) - L_{2,i}(k)}{2 \times VHTLTF(k)} \\ \hat{h}_{i\,2}(k) &= \frac{L_{1,i}(k) + L_{2,i}(k)}{2 \times VHTLTF(k)} \end{aligned} \tag{3.13}$$

When $N_{STS} = 3$, there are four transmitted VHT-LTFs and the channel estimation for this case (e.g., 3×3 MIMO system) is as follows,

$$\begin{aligned} \hat{h}_{i\,1}(k) &= \frac{L_{1,i}(k) - L_{2,i}(k)}{2 \times VHTLTF(k)} \\ \hat{h}_{i\,2}(k) &= \frac{L_{1,i}(k) - L_{3,i}(k)}{2 \times VHTLTF(k)} \\ \hat{h}_{i\,3}(k) &= \frac{L_{1,i}(k) - L_{4,i}(k)}{2 \times VHTLTF(k)} \end{aligned} \tag{3.14}$$

And finally for $N_{STS} = 4$ all the four transmitted VHT-LTFs are used for the channel estimation of every path as follows,

$$\begin{aligned} \hat{h}_{i\,1}(k) &= \frac{L_{1,i}(k) - L_{2,i}(k) + L_{3,i}(k) + L_{4,i}(k)}{4 \times VHTLTF(k)} \\ \hat{h}_{i\,2}(k) &= \frac{L_{1,i}(k) + L_{2,i}(k) - L_{3,i}(k) + L_{4,i}(k)}{4 \times VHTLTF(k)} \\ \hat{h}_{i\,3}(k) &= \frac{L_{1,i}(k) + L_{2,i}(k) + L_{3,i}(k) - L_{4,i}(k)}{4 \times VHTLTF(k)} \\ \hat{h}_{i\,4}(k) &= \frac{-L_{1,i}(k) + L_{2,i}(k) + L_{3,i}(k) + L_{4,i}(k)}{4 \times VHTLTF(k)} \end{aligned} \tag{3.15}$$

Since pilots are identical on all streams, they are not orthogonal to each other, and the channel estimation for the pilot sub-carriers can not be estimated using the VHT-LTF as the other sub-carriers. Instead, interpolation between the surrounding sub-carriers is used to estimate the channel for the pilot sub-carriers. In this receiver cubic interpolation was used. It is the simplest method that offers true continuity between the segments. Cubic interpolation requires four sub-carriers surrounding the pilot sub-carrier, two on each side. The channel estimation of a pilot sub-carrier is

$$\hat{h}_{ij}(k_p) = \frac{1}{2^3}a_0 + \frac{1}{2^2}a_1 + \frac{1}{2}a_2 + a_3 \tag{3.16}$$

where k_p is the pilot sub-carrier number, and a_0, a_1, a_2 and a_3 are,

$$\begin{aligned} a_0 &= \hat{h}_{ij}(k_p+2) - \hat{h}_{ij}(k_p+1) - \hat{h}_{ij}(k_p-1) + \hat{h}_{ij}(k_p-2) \\ a_1 &= \hat{h}_{ij}(k_p-2) - \hat{h}_{ij}(k_p-1) - a_0 \\ a_2 &= \hat{h}_{ij}(k_p+1) - \hat{h}_{ij}(k_p-2) \\ a_3 &= \hat{h}_{ij}(k_p-1) \end{aligned} \tag{3.17}$$

The estimated channel matrix $\hat{H}(k)$ is not perfect and can be modelled as

$$\hat{H}(k) = H(k) + E(k) \tag{3.18}$$

where $E(k)$ is an estimation error.

3.3.3 Equalizer

A Zero-Forcing equalizer was used in the receiver, it is a linear equalization algorithm that applies an inverse of the frequency response of the the channel to the received signal. The linear zero-forcing $M \times N$ matrix filter $G(k)$ is given by the pseudo-inverse [13]

$$G(k) = H^{\dagger}(k) = \Big(H^{*}(k)H(k)\Big)^{-1}H^{*}(k) \tag{3.19}$$

where $*$ stands for Hermitian transpose. The estimated zero-forcing matrix can be modelled as

$$\hat{G}(k) = \hat{H}^{\dagger}(k) = H^{\dagger}(k) + \Omega(k) \tag{3.20}$$

where $\Omega(k)$ is the contribution of the estimation error in the pseudo-inverse. The original transmitted signal can be estimated in the receiver as

$$\hat{S}(k) = \hat{G}(k)R(k) \tag{3.21}$$

substituting (2.1) and (3.20) in (3.21)

$$\begin{aligned} \hat{S}(k) &= \hat{G}(k)\Big(H(k)S(k) + n(k)\Big) \\ \hat{S}(k) &= S(k) + \Omega(k)S(k) + \hat{H}^{\dagger}(k)n(k) \end{aligned} \tag{3.22}$$

if $\Omega(k)S(k) << 1$, then it can be approximated as

$$\hat{S}(k) \approx S(k) + \hat{H}^{\dagger}(k)n(k) \tag{3.23}$$

The zero-forcing equalizer removes all ICI, and is ideal when the channel is noiseless. However, when the channel is noisy, the zero-forcing equalizer will amplify the noise greatly at frequencies where the channel response has a small magnitude in the attempt to invert the channel completely. Zero-forcing equalizer is sufficient for the purposes of this simulation, but a more balanced linear equalizers should be used in a real application (e.g., MMSE).

The equalizer transforms a number of multiplexed received chains N_{RX} into a number of equalized space-time streams N_{STS}. Each space-time stream passes a pilot tracker, which reads the pilot sub-carriers in each OFDM symbol, and then uses the pilots to correct for any frequency offset that may occur during long bursts.

3.3.4 Deparsing and Decoding

The outputs of the equalizer and the pilot trackers are input to the STBC decoder, it inverts the process of the STBC encoder in subsection 3.2.11.When the STBC option is used during transmission, the STBC decoder combines every two copies of the received signal (space-time streams) into a single spatial stream, improving the reliability of the data transfer [14].

The receiver segment parser and segment deparser reverts the processes of the transmitter parsers (subsection 3.2.6). Every spatial stream is split into two segments in case of using the 160 MHz or the non-contiguous 80+80 MHz bandwidths.

The deinterleaver inverts the procedure of the interleaver, while the demodulator extracts the original transmitted bits from the received modulated constellations. The demodulated bits are then passed through the stream deparser, it distributes blocks of bits form the spatial streams into a number of decoders equivalent to the number of encoders used in the transmitter.

The data bits are depunctured by inserting dummy zeros in the locations where encoded bits where punctured. Then they are passed through the Viterbi decoder[2]. The Viterbi decoder is widely used to decode bit streams that have been encoded with a convolutional code [15, 3]. A hard decision decoder was used in this receiver, where it receives a simple bit stream on its input, and a Hamming distance is used as a metric.

An encoder deparser combines the outputs of the decoders into one stream in a Round-Robin fashion. Then a descrambler return the decoded data bits into their original form, and finally, the padding bits are removed, and the PSDU is delivered to the receiver.

[2]The Viterbi algorithm is recommended by the IEEE for decoding 11ac frames [2].

Chapter 4

Simulation Environment

The simulations created for this thesis were done in MATLAB. It is built on an existing 11n standard simulation for a SISO system with a 20 MHz channel bandwidth. In order to help understanding and debugging the code, the usage of MATLAB's specialised functions and tool boxes was minimised; basic functions were used instead to create the simulation blocks. The final simulation program was verified with the official IEEE 802.11ac waveform generator, and showed positive results.

The data bits are represented in matrices. During all the processes and states, the rows are used to represent symbols, columns are used for sub-carriers, and finally the third dimension is used for representing different streams (see Figure 4.1). In the case of 160 MHz bandwidth, a fourth dimension is used to represent the two segments.

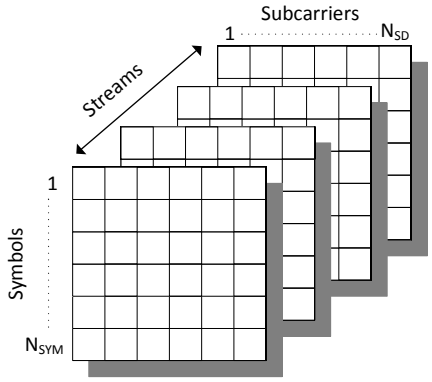

Figure 4.1: Representing data bits in MATLAB matrices.

The simulation supports the 11a, 11n and 11ac standards with a wide range of settings. A block diagram showing the main loop of the simulation is shown in Figure 4.2. The following subsections explain every block in

more details.

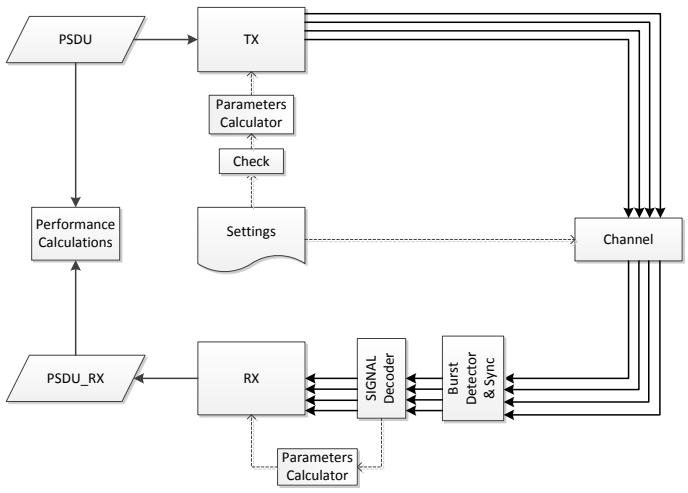

Figure 4.2: Block diagram of the simulation.

4.1 Settings and Parameters

The settings of the simulation are input in a special file that is read at the start of the run. Most of these settings are the fields of the TXVECTOR as specified in [5, 2]. The different WLAN standards have different fields in the TXVECTOR. Table 4.1 demonstrates some important fields of the TXVECTOR, used in the 11ac case. In addition to the TXVECTOR parameters that mainly affect the transmitter, other settings are used in order to describe the channel and the number of antennas in the receiver.

Table 4.1: Important 11ac TXVECTOR fields.

Field Name	**Range**	**Description**
N_TX	1 to 8	Number of transmitter antennas
FEC_CODING	0, 1	BCC (0) or LDPC(1)
STBC	0, 1	Using STBC (1)
GI_TYPE	0, 1	Long GI (0), Short GI (1)
MCS	0 to 9	Modulation and coding scheme
CH_BANDWIDTH	20, 40, 80, 160	Channel bandwidth (MHz)
NUM_STS	1 to 8	Number of space-time streams
PSDU_LENGTH	1 to 1048575	Length of the PSDU

Table 4.2: Calculated parameters.

Symbol	Description
N_{SS}	Number of spatial streams
N_{STS}	Number of space-time streams
N_{TX}	Number of transmitter chains
N_{SD}	Number of data sub-carriers
N_{SP}	Number of pilot sub-carriers
N_{BPSC}	Bits per sub-carrier
N_{BPSCS}	Bits per sub-carrier per spatial stream
N_{CBPS}	Codded bit per symbol
N_{CBPSS}	Codded bits per symbol per spatial stream
N_{CBPSSI}	Coded bits per symbol per spatial stream per BCC interleaver block
N_{DBPS}	Data bit per symbol
N_{Mod}	Modulation scheme
N_{Rate}	Coding rate
N_{FFT}	FFT size
N_{FS}	Sampling rate
N_{GI}	GI length
N_{ES}	Number of encoders
N_{VHTLTF}	Number of VHT-LTFs in frame
N_{FIELD}^{TONE}	Scaling factors
N_{LENGTH}	Data length
N_{SYM}	Number of symbols
N_{PAD}	Padding length

The program checks the validity of the settings, and makes sure they are within the supported ranges. Some combinations of settings are not allowed according to the IEEE standards. The check function gives proper warnings to the user when a problem is encountered, or a range is exceeded.

The next block is the parameters calculator. This block contains functions that translate the TXVECTOR fields into useful parameters that can be utilised in generating the transmitted frame[1]. The list of calculated parameters for the 11ac case is shown in Table 4.2.

4.2 Transmitter

The PSDU in this simulation is random generated data that is fed to the transmitter. The transmitter modulates the PSDU as described in sec-

[1] This block is also reused at the receiver side to extract parameters from the received RXVECTOR

tion 3.2. Depending on the operating mode and the calculated parameters, it generates SISO/MIMO frames containing preambles and DATA symbols. The output of the transmitter is a number a base signals, represented in time domain as matrices of complex bits. The transmitter output is fed to the channel.

4.3 Channel

The channel block simulates the effects of analogue/digital conversions, MIMO multiplexing, frequency and phase offsets, time delay, and AWGN. The MIMO multiplexing is done by multiplying the transmitted streams by a channel matrix H. A random generated frequency non-selective channel matrix was used in all the simulations of this thesis, the 4×4 version of it is in (4.1).

$$H = \begin{bmatrix} +0.10 + 0.20j & -0.06 + 0.04j & +0.15 + 0.10j & -0.13 - 0.04j \\ -0.18 - 0.28j & -0.09 + 0.12j & +0.21 + 0.17j & -0.06 - 0.19j \\ +0.18 - 0.01j & -0.08 - 0.27j & -0.04 + 0.05j & +0.04 - 0.19j \\ -0.30 - 0.01j & +0.22 - 0.09j & -0.22 + 0.20j & -0.13 + 0.10j \end{bmatrix} \tag{4.1}$$

The channel block, adds AWGN according to the SNR values specified in the setting file, as well as the frequency, phase and time offsets. The real and imaginary parts of an estimated 2×2 MIMO channel response are shown in Figure 4.3.

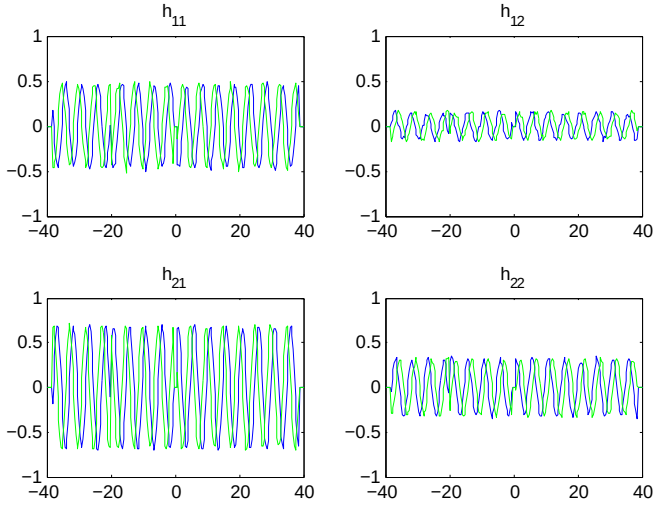

Figure 4.3: Estimated 2×2 MIMO channel response, real part in blue, and imaginary part in green.

Table 4.3: IEEE standards (frame formats) and the required SIGNAL fields.

IEEE standard	Required SIGNAL fields
11a	L-SIG
11n Legacy	L-SIG
11n Mixed Mode	L-SIG, HT-SIG
11n Green Field	HT-SIG
11ac	L-SIG, VHT-SIG-A, VHT-SIG-B

4.4 Receiver

The burst detector and synchronisation block triggers the start of the frame as explained in subsection 3.3.1. It corrects for the frequency and phase offsets, then passes the received streams to the SIGNAL decoder. The frame format is detected, and then the corresponding SIGNAL fields (Table 4.3) are decoded in order to extract the RXVECTOR. In addition, the SIGNAL decoder performs different CRCs depending on the IEEE standard in use, to confirm correct reception of the transmitted frame. The RXVECTOR is passed through the parameters calculator block, and finally the corrected streams are sent to the main receiver block along with the calculated parameters. The received distorted constellation of 3×3 MIMO 16-QAM system with SNR = 25 dB are shown in Figure 4.4. And the received signal spectrum of a 80 MHz system is shown in Figure 4.5. The receiver block estimates the channel and then extracts the PSDU from the received streams as explained in section 3.3.

4.5 Performance Calculations

The BER and EVM are calculated by comparing the transmitted PSDU and constellations with the received ones for a range of SNR values. The performance calculations are done by automating the program to run a Monte Carlo simulation. A frame that carries a PSDU with a fixed length of 15000 bits was used; the frame is transmitted through the channel 10000 times (channel realizations) for every SNR value. These measurements were repeated with different settings, to compare and study the performance of the 11ac standard in different operating modes.

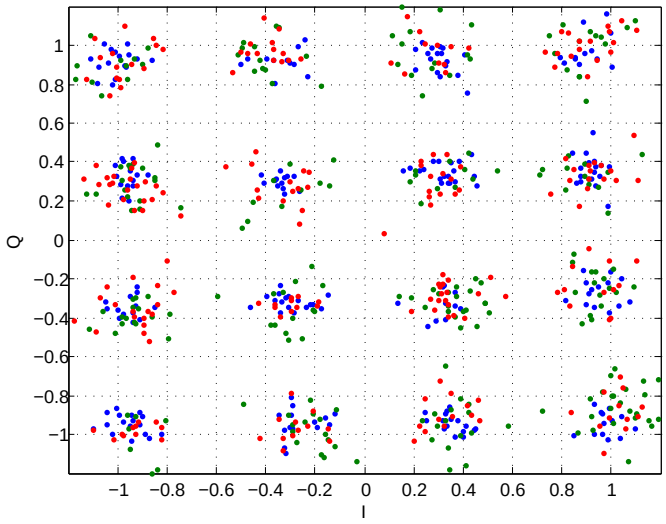

Figure 4.4: Constellation of a 3×3 MIMO 16-QAM received signal, SNR = 25 dB, colours represent different streams.

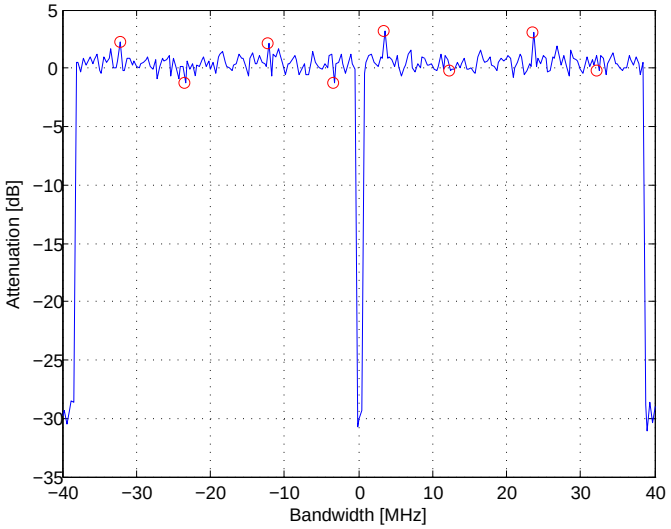

Figure 4.5: 80 MHz received signal spectrum, pilots' sub-carriers are marked with red circles.

Chapter 5

Performance Analysis

5.1 BER Analysis

The Bit Error Rate is a unitless performance measure, where the number of bit errors (accrued during transmission through the channel) is divided by the total number of transmitted bits. BER assesses the full end to end performance of a system including the transmitter, receiver and the medium between the two.

The energy per bit to noise power spectral density ratio E_b/N_0 is a normalized SNR measure, also known as the "SNR per bit". It is useful when comparing the BER performances of different digital modulation schemes and coding rates. The E_b/N_0 in the simulations of this thesis was calculated by converting the channel SNR as

$$E_b/N_0 = SNR \times \frac{N_{FFT}}{N_{SD}} \times \frac{T_{FFT} + T_{GI}}{T_{FFT}} \times \frac{1}{N_{SS}} \times \frac{1}{N_{Rate}} \times \frac{1}{log_2(M)} \quad (5.1)$$

where, $\frac{N_{FFT}}{N_{SD}}$ is the ratio of the used data sub-carriers to the total number sub-carriers. And $\frac{T_{FFT} + T_{GI}}{T_{FFT}}$ compensates for the bandwidth wasted for the GI; T_{FFT} is the FFT period, and T_{GI} is the GI period. M is the modulation constellations size. By defining the data rate as

$$f_b = BW \times \frac{N_{SD}}{N_{FFT}} \times \frac{T_{FFT}}{T_{FFT} + T_{GI}} \times N_{SS} \times N_{Rate} \times log_2(M) \quad (5.2)$$

substituting (5.2) in (5.1), E_b/N_0 can be calculated as

$$E_b/N_0 = SNR \times \frac{BW}{f_b} \quad (5.3)$$

Pre-calculated data rate tables are available in [2] for all combinations of settings. These tables were used for the E_b/N_0 conversions.

Table 5.1: MCSs parameters used in simulations.

MCS Number	Modulation	Coding Rate
MCS 0	BPSK	1/2
MCS 2	QPSK	3/4
MCS 4	16-QAM	3/4
MCS 7	64-QAM	5/6
MCS 8	256-QAM	3/4

The BER performance of different Modulation and Coding Schemes was studied, where five different combination of settings were compared. Table 5.1 describes the parameters of the used MCSs. The BER plots of the five studied MCSs for 2×2 MIMO system are shown in Figure 5.1.

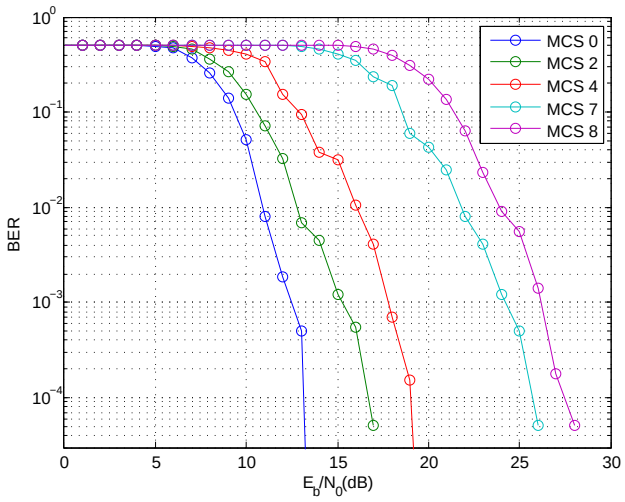

Figure 5.1: BERs for different MCSs in a 2×2 sytem, BW = 80 MHz.

The BPSK modulation requires the lowest SNR, followed by QPSK, 16-QAM, 64-QAM and finally the 256-QAM. The Forward Error Correction Codes used causes the sharp drop in the curves when compared with standard uncoded BERs plots.

The Error Vector Magnitude (EVM) is a measure of how far the constellation points are from the ideal locations. It is the average Root Mean Square (RMS) power of the error vector, normalized to signal power [16]. It can be defined as

$$EVM_{RMS} = \left[\frac{\frac{1}{T} \sum_{r=1}^{T} \left(\left| I_r - \tilde{I}_r \right|^2 + \left| Q_r - \tilde{Q}_r \right|^2 \right)}{P_0} \right]^{\frac{1}{2}} \tag{5.4}$$

where T is the total number of constellations, I_r and Q_r are the in-phase and quadrature components of the measured r^{th} sample respectively. P_0 is the normalized mean-square amplitude of the constellations. The EVM can be expressed in dB. Figure 5.2 shows the EVM of 2×2 MIMO system.

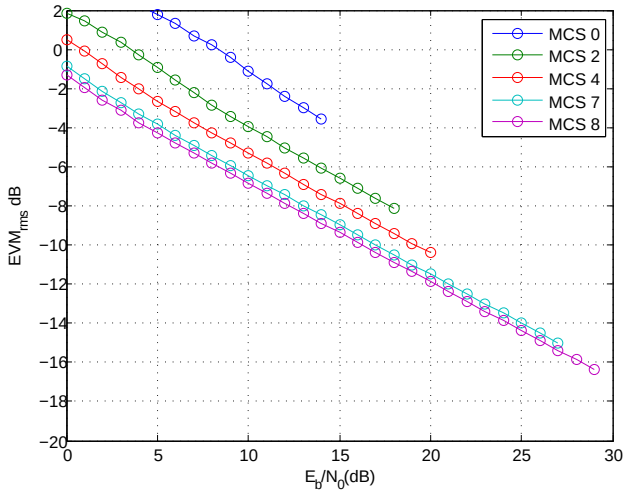

Figure 5.2: BERs for different MCSs in a 2×2 sytem, BW = 80 MHz.

The separation between different MCS curves is due to the difference in the number bits carried by each constellation point. Higher order of modulations shows less EVM.

5.2 SISO vs. MIMO

A BER performance comparison between a SISO system, a 2×2, a 3×3, and a 4×4 MIMO systems is shown in Figure 5.3. The 4×4 case shows the highest sensitivity to noise, followed by the 3×3 and then 2×2 cases. The SISO system showed an unexpected performance exceeding that of the 2×2 system. The reason is due to the ideal non-multiplexing channel experienced by the SISO signal. In a real air-interface application, the SISO system is expected to show better performance than any comparable MIMO system.

The results in Figure 5.3 are for a 80 MHz bandwidth system, with MCS = 8 (256-QAM, 3/4 coding rate). The same simulation was repeated for different combinations of bandwidths and MCSs. The results showed similar orders of the SISO and MIMO cases, and therefore were not included.

5.3 STBC Performance

The STBC is one of the main features in the IEEE 802.11 standards. A simulation was run to compare the performance of a system employing the

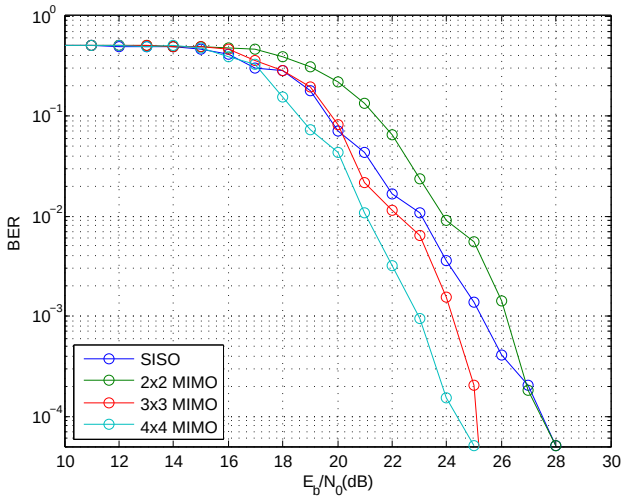

Figure 5.3: BER for different MIMO and SISO systems, BW = 80 MHz, MCS = 8.

STBC feature with one that does not. Figure 5.4 shows this BER comparison, between a normal 2×2 MIMO system, and a STBC enabled system. Note that when the STBC feature is in use, it actually expand the 2 available spatial streams into 4 space-time streams.

This simulation was run for three different MCSs in a 80 MHz system. The separation between curves of similar MCS, presents an enhancements in the performance of the STBC enabled systems. The difference expands with higher E_b/N_0 values and averages to 3 dB, as expected when doubling the number os streams.

5.4 Bandwidth Effect

The effect of channel bandwidth was studied by running a simulation to compare identical systems with different channel bandwidths. A BER performance comparison between a 20, 40, 80, and 160 MHz systems is shown in Figure 5.5.

The compared systems shows similar performances with slight differences. The difference could be related to the ratio of pilot sub-carriers to data sub-carriers in different bandwidth systems. This simulation was run for a MCS = 7; other tested MCSs showed very similar results.

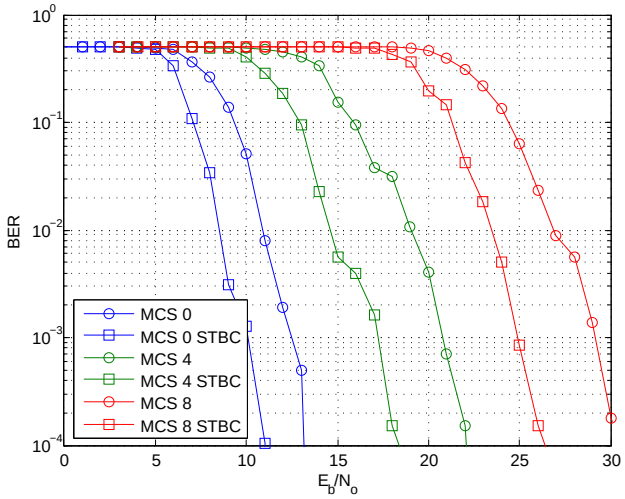

Figure 5.4: The effect of STBC on BER of a 2×2 MIMO system, BW = 80 MHz.

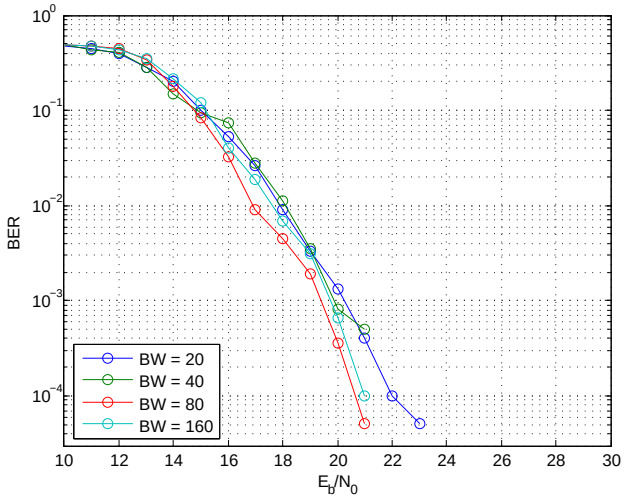

Figure 5.5: Effect of BW on BER, 4×4 MIMO system, MCS = 7.

Chapter 6

Conclusion

This work studies the physical layer of the under-development new WLAN standard, IEEE 802.11ac. The new standard promises high reliable data rates exceeding the 1 Gbps limit. This will be mainly achieved by employing more bandwidth, higher orders of modulations, and more MIMO streams. These new technologies face great challenges, including, higher hardware requirements, backward compatibility and keeping a low cost.

The 11ac is compatible with the 11n and 11a standards. They all operate in the same below 6 GHz band and use OFDM methods. Both the 11ac and the 11n standards benefit from MIMO and STBC techniques.

The 11ac PHY frame consists of many preamble fields followed by the data symbols. Each field is built by the transmitter to serve a specific purpose. Some fields carry information about the transmitted frame, and others are used for channel estimations. The transmitted data is encoded with different techniques and operations to add robustness; these operations are inverted at the receiver side to extract the data back.

MATLAB is a powerful tool, it simplifies scientific programming by using matrix operations. MATLAB was used to create a simulation environment for the 11ac PHY. All the standard mandatory features were included in addition to a big portion of the optional features. The simulation was used to study the performance of the 11ac standard. BER calculation were measured for a frequency non-selective AWGN MIMO channel.

The BER performance of different MCS shows that higher orders of modulation require lower noise level (Higher SNR). While these same modulations maintain a low EVM, when the comparison is done per bit.

Higher orders of MIMO systems show better BER performance than others, although the usage of such systems may require higher SNR values in real applications.

The STBC can achieve better performance when used. When compared with a similar system that is not using this feature; it can achieve 3 dB enhancement in BER performance.

The type of channel bandwidth used in 11ac have a very slight effect on the BER performance of the system, while it is a key factor in achieving higher data rates.

6.1 Future Work

The 11ac simulations in this thesis were all done in a virtual MATLAB environment. A hardware air-interface simulations could be carried on. This can be achieved by using specialised arbitrary waveform generator, antennas, and a specialised spectrum analyser. After preparing the physical setup, the simulation can be automated by a MATLAB script.

In the study of the 11ac performance, only symmetrical MIMO systems were considered, 2×2, 3×3, and 4×4. Other combinations can be tested and compared. For example, studying the effect of the number of antennas in the receiver or in the transmitter.

The simulations in this thesis covers a wide range of optional features in the 11ac standard. But more features could be added to include up to 8 spatial streams, and beamforming. The beamforming feature, helps the access point to direct the transmitter smart antenna beam to achieve better coverage and wider range. This is done by communicating with the stations, and acquiring information about the required direction in smart methods. These features can be added to the simulation and tested with different settings for optimisation.

References

[1] L. Garber, "Wi-Fi races into a faster future," *Computer*, vol. 45, pp. 13–16, Mar. 2012.

[2] "IEEE draft standard for IT - telecommunications and information exchange between systems - LAN/MAN - specific requirements - part 11: Wireless LAN medium access control and physical layer specifications - amd 4: Enhancements for very high throughput for operation in bands below 6GHz," *IEEE P802.11ac™/D3.0*, pp. 1–385, June 2012.

[3] J. G. Proakis and M. Salehi, *Digital Communication.* New York McGraw Hill, 5 ed., 2007.

[4] T. K. Paul and T. Ogunfunmi, "Wireless LAN comes of age: Understanding the IEEE 802.11n amendment," *Circuits and Systems Magazine, IEEE*, vol. 8, pp. 28–54, Mar. 2008.

[5] "IEEE standard for IT - telecommunications and information exchange between systems - LAN/MAN - specific requirements - part 11: Wireless LAN medium access control and physical layer specifications," *IEEE Draft P802.11-REVmb™/D10.0*, pp. 1–3026, Aug. 2011.

[6] S. M. Alamouti, "A simple transmit diversity technique for wireless communications," *Selected Areas in Communications, IEEE Journal on*, vol. 16, pp. 1451–1458, Oct. 1998.

[7] H. Ochi and W. A. Syafel, "PAPR reduction for very high throughput WLAN with backward compatibility to IEEE 802.11 a/n," *Majalah Transmisi*, vol. 11, pp. 113–117, Sept. 2009.

[8] M. N. Ellanti, S. S. Gorshe, L. G. Raman, and W. D. Grover, *Next Generation Transport Networks: Data, Management, and Control Planes.* Springer, 1 ed., Apr. 2005.

[9] C.-H. Liu, "On the design of OFDM signal detection algorithms for hardware implementation," in *Global Telecommunications Conference. GLOBECOM '03. IEEE*, vol. 2, pp. 596–599, Dec. 2003.

[10] T. M. Schmidl and D. C. Cox, "Robust frequency and timing synchronization for OFDM," *IEEE Transactions on Communications*, vol. 45, pp. 1613–1621, Dec. 1997.

[11] J. J. van de Beek, M. Sandell, and P. O. Borjesson, "ML estimation of time and frequency offset in OFDM systems," *IEEE Transactions on Signal Processing*, vol. 45, pp. 1800–1805, July 1997.

[12] C.-H. Lin, R. C.-H. Chang, K.-H. Lin, and Y.-Y. Lin, "Implementation of channel estimation for MIMO-OFDM systems," in *SoC Design Conference (ISOCC), 2010 International*, pp. 99–102, Nov. 2010.

[13] S. G. Kim, D. Yoon, S. K. Park, and Z. (Daniel) Xu, "Performance analysis of the MIMO zero-forcing receiver over continuous flat fading channels," in *3rd International Conference on Information Sciences and Interaction Sciences (ICIS)*, pp. 324–327, June 2010.

[14] U. Madhow, *Fundamentals of Digital Communication*. Cambridge University Press, 2008.

[15] A. Viterbi, "Error bounds for convolutional codes and an asymptotically optimum decoding algorithm," *IEEE Transactions on Information Theory*, vol. 13, pp. 260–269, Apr. 1967.

[16] Z. Qijun, X. Qinghua, and Z. Wei, "Notice of violation of IEEE publication principles a new EVM calculation method for broadband modulated signals and simulation," in *8th International Conference on Electronic Measurements and Instruments. ICEMI.*, pp. 661–665, July 2007.